Chemistry of Polynuclear Metal Complexes with Bridging Carbene or Carbyne Ligands. Part 89.[1] Tetra- and Penta-nuclear Tungsten–Rhodium Complexes: Crystal Structures of $[W_3Rh_2(\mu\text{-}CO)_2(\mu\text{-}CMe)\{\mu\text{-}C(Me)C(O)\}(\mu\text{-}PPh_2)_2(\mu_3\text{-}CMe)(CO)_2(\eta\text{-}C_5H_5)_3]$ and $[W_3Rh_2(\mu\text{-}CO)_3(\mu\text{-}CMe)\{\mu\text{-}C(Me)PPh_2\}(\mu_3\text{-}CMe)(CO)_2(\eta\text{-}C_5H_5)_3]$ *

Simon J. Davies, Judith A. K. Howard, Massimino U. Pilotti, and F. Gordon A. Stone
Department of Inorganic Chemistry, The University, Bristol BS8 1TS

Treatment of $[Rh_2(\mu\text{-}PPh_2)_2(cod)_2]$ (cod = cyclo-octa-1,5-diene) in thf (tetrahydrofuran) at room temperature with 2 equivalents of $[W(\equiv CMe)(CO)_2(\eta\text{-}C_5H_5)]$ rapidly affords the tetranuclear metal complex $[W_2Rh_2(\mu\text{-}CMe)_2(\mu\text{-}PPh_2)_2(CO)_4(\eta\text{-}C_5H_5)_2]$ (**4**). If the same reaction is carried out using an excess of the ethylidynetungsten complex two metal cluster compounds are obtained: $[W_2Rh_2(\mu\text{-}CO)\{\mu\text{-}C(Me)C(O)\}(\mu\text{-}PPh_2)_2(\mu_3\text{-}CMe)(CO)_2(\eta\text{-}C_5H_5)_2]$ (**5**) (formed as a separable mixture of two diastereoisomers) and $[W_3Rh_2(\mu\text{-}CO)_2(\mu\text{-}CMe)\{\mu\text{-}C(Me)C(O)\}(\mu\text{-}PPh_2)_2(\mu_3\text{-}CMe)(CO)_2(\eta\text{-}C_5H_5)_3]$ (**6**). The structure of the latter was established by *X*-ray diffraction. The molecule has an essentially planar W(1), Rh(1), W(2), Rh(2), W(3) framework. Carbonyl groups bridge the Rh(1)–W(1) and Rh(2)–W(2) bonds, and PPh_2 ligands span the Rh(1)–W(2) and Rh(2)–W(3) linkages. Ethylidyne groups edge-bridge the Rh(1)–W(1) bond and triply bridge the atoms Rh(1)W(2)Rh(2), but the Rh(1) ··· Rh(2) separation [3.115(4) Å] is non-bonding. The Rh(2)–W(3) bond is bridged by a C(Me)C(O) ketenyl group, and the terminal W atoms in the chain each carry a CO ligand and a C_5H_5 ring. A third C_5H_5 group ligates W(2). The metal–metal distances fall into two groups [Rh(1)–W(2) 2.791(6), Rh(2)–W(3) 2.813(4); and Rh(1)–W(1) 2.696(5), Rh(2)–W(2) 2.664(5) Å], with the shorter separations corresponding to double bonds and the longer to single bonds. Compound (**6**) is produced by addition of a molecule of $[W(\equiv CMe)(CO)_2(\eta\text{-}C_5H_5)]$ to (**5**), while the latter is formed by isomerisation of (**4**), a process necessitating migration of μ-CMe and $\mu\text{-}PPh_2$ between the metal centres. After several hours solutions of (**6**) in thf afford quantitatively the complex $[W_3Rh_2(\mu\text{-}CO)_3(\mu\text{-}CMe)\{\mu\text{-}C(Me)PPh_2\}(\mu\text{-}PPh_2)(\mu_3\text{-}CMe)(CO)_2(\eta\text{-}C_5H_5)_3]$ (**7**) an isomer of (**6**). The structure of (**7**) was established by *X*-ray diffraction. An essentially planar metal atom chain W(1), Rh(1), W(2), Rh(2), W(3) forms the spine of the molecule. The various ligands ligate the rhodium and tungsten atoms in a similar manner to those in (**6**), with the exception of the groups which span the Rh(2)–W(3) bond. This bond is now bridged by a λ^5-phospha-alkyne $C(Me)PPh_2$ fragment such that the phosphorus atom ligates W(3) and the carbon atom *C*Me is bonded to Rh(2) and W(3). The Rh(2)–W(3) bond is also bridged by a CO ligand. Thus the conversion of (**6**) into (**7**) involves a novel interchange of CO and PPh_2 fragments such that in the former a μ-C(Me)C(O) group is present and in the latter a $\mu\text{-}C(Me)PPh_2$ moiety. The n.m.r. data (^1H, $^{13}C\text{-}\{^1H\}$, and $^{31}P\text{-}\{^1H\}$) for the new compounds are reported and discussed.

During the last two decades most of the major advances in metal cluster chemistry have been associated with the discovery of large numbers of species having polyhedral arrays of metal atoms.[2] Usually these polyhedra have triangulated faces. Cluster compounds with structures based on a chain of metal atoms have been less well investigated.[3] However, in a series of recent articles[4] we have described the rational directed synthesis of chain-like metal clusters in which the spines of the molecules consist of tungsten or molybdenum atoms linked to platinum or nickel.

The procedure used in these syntheses involves displacement of labile cod (cyclo-octa-1,5-diene) ligands from the complexes $[Ni(cod)_2]$ or $[Pt(cod)_2]$ by the alkylidynemetal compounds $[M(\equiv CR)(CO)_2(\eta\text{-}C_5R'_5)]$ (M = Mo or W, R = alkyl or aryl, R′ = H or Me), followed by sequential addition of these same reagents to the initially formed products. For example, treatment of $[Pt(cod)_2]$ in ethylene-saturated light petroleum solutions with 2 equivalents of $[W(\equiv CR)(CO)_2(\eta\text{-}C_5H_5)]$ ($R = C_6H_4Me$-4) yields the trimetal complex $[W_2Pt(\mu\text{-}CR)_2(CO)_4(\eta\text{-}C_5H_5)_2]$ (**1**). The latter is unsaturated and will combine with $[Pt(cod)_2]$ to afford products in which a Pt(cod) fragment is co-ordinated to one or both of the C=W groups. With 1 equivalent $[Pt(cod)_2]$ the tetranuclear cluster $[W_2Pt_2(\mu\text{-}CR)(\mu_3\text{-}CR)(CO)_4(cod)(\eta\text{-}C_5H_5)_2]$ (**2**) is produced. Displacement of the terminal cod group in the latter is possible by further addition of $[W(\equiv CR)(CO)_2(\eta\text{-}C_5H_5)]$, thereby generating the pentanuclear metal cluster $[W_3Pt_2(\mu\text{-}CR)_2(\mu_3\text{-}CR)(CO)_6(\eta\text{-}C_5H_5)_3]$ (**3**). Many syntheses have been based on an extension of these principles.[4] Recently

---

* 1,2;3,4-Di-μ-carbonyl-1,5-dicarbonyl-1,3,5-tris(η-cyclopentadienyl)-2,3;4,5-bis(μ-diphenylphosphido)-1,2-μ-ethylidyne-2,3,4-μ_3-ethylidyne-4,5-μ-[1′-oxopropen-2-yl-$C^1(W^5)C^2(W^5Rh^4)$]- and 1,2;3,4;4,5-tri-μ-carbonyl-1,5-dicarbonyl-1,3,5-tris(η-cyclopentadienyl)-4,5-μ-[1′,1′-diphenyl-(λ^5-phosphapropene-1,2-diyl-$C^2(Rh^4)P(W^5)$]-2,3-μ-diphenylphosphido-1,2-μ-ethylidyne-2,3,4-μ_3-ethylidyne-2,4-dirhodium-1,3,5-tritungsten.

Supplementary data available: see Instructions for Authors, *J. Chem. Soc., Dalton Trans.*, 1989, Issue 1, pp. xvii—xx.

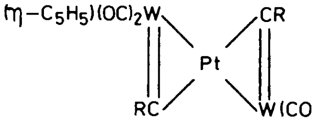

(1)

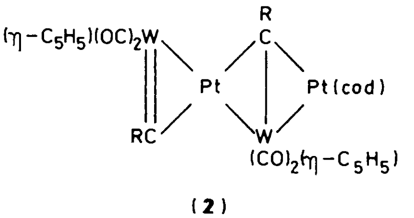

(2)

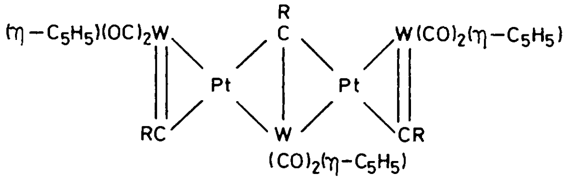

(3)

R = C_6H_4Me-4

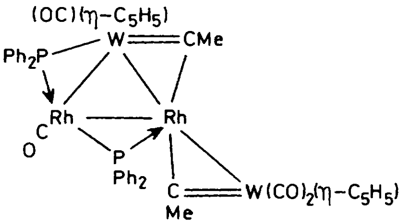

(4)

compounds have been structurally characterised having as many as eleven metal atoms in the spine of the molecules.[4e]

In an attempt to extend the range of transition metals which might be incorporated in chain structures with tungsten, we have investigated the reaction between [Rh_2(μ-PPh_2)$_2$(cod)$_2$] and [W(≡CMe)(CO)$_2$(η-C_5H_5)]. The dirhodium compound contains terminal cod ligands,[5] and it was anticipated that these groups might be displaced by treatment with 2 equivalents of the tungsten reagent so as to form a cluster having the core structure W(μ-CMe)Rh(μ-PPh_2)$_2$Rh(μ-CMe)W. The terminal C=W groups in the latter might then be points of attachment for other metal–ligand fragments. Although a reaction readily occurred between [Rh_2(μ-PPh_2)$_2$(cod)$_2$] and [W(≡CMe)(CO)$_2$(η-C_5H_5)], the nature of the products obtained was unexpected as a result of migration of CO and μ-PPh_2 groups between the metal centres. A preliminary account of some of the work described herein has been given.[6]

Results and Discussion

Addition of 2 equivalents of [W(≡CMe)(CO)$_2$(η-C_5H_5)] to [Rh_2(μ-PPh_2)$_2$(cod)$_2$] in tetrahydrofuran (thf) at room temperature resulted in the mixture rapidly changing colour from green to dark brown. Monitoring by i.r. spectroscopy revealed that within 10 min all the tungsten reagent had been consumed. The product [W_2Rh_2(μ-CMe)$_2$(μ-PPh_2)$_2$(CO)$_4$(η-C_5H_5)$_2$] (4) was isolated by column chromatography on alumina, and data for this complex are given in Tables 1—3.

The spectroscopic properties are in agreement with the structure proposed. The ^{31}P-{^{1}H} n.m.r. spectrum (Table 3) was especially informative. There was a peak at δ 271.2 p.p.m., appearing as an apparent triplet of doublets, and a resonance at δ 162.2 p.p.m. which was a doublet of doublets. Both signals are in the chemical shift range expected for a μ-PPh_2 group spanning a metal–metal bond,[7] but clearly the Rh(μ-PPh_2)$_2$Rh symmetry present in the precursor had been lost. The large ^{31}P–^{31}P coupling constant (132 Hz) associated with the two resonances implies a transoid P–Rh–P arrangement at one of the rhodium centres. A comparison may be made with the ^{31}P–^{31}P coupling (103 Hz) in the ^{31}P-{^{1}H} n.m.r. spectrum of the irondirhodium compound [$FeRh_2$(μ-CO)$_2$(μ-PBu^t_2)$_2$(CO)$_3$($PHBu^t_2$)].[8] The latter has a structure based on a metal triangle with μ-phosphido ligands transoid to one another.

Since the resonance at δ 271.2 p.p.m. in the ^{31}P-{^{1}H} n.m.r. spectrum of complex (4) shows two other couplings, apart from that to the other ^{31}P signal, it must correspond to a μ-PPh_2 fragment bridging two inequivalent rhodium atoms. The resonance appears as an apparent triplet of doublets because one of the ^{103}Rh–^{31}P coupling constants is identical with the ^{31}P–^{31}P coupling constant. The resonance at δ 162.2 p.p.m. shows only one ^{103}Rh–^{31}P coupling (98 Hz) in agreement with the second phosphido group bridging a Rh–W bond.

The ^{13}C-{^{1}H} n.m.r. spectrum of complex (4) shows resonances due to μ-C nuclei at δ 349.1 and 346.5 p.p.m., both appearing as doublets of doublets due to ^{31}P and ^{103}Rh coupling. These signals appear in the chemical shift range (300—400 p.p.m.) expected for alkylidyne ligands edge-bridging a metal–metal bond.[9] Thus in the ^{13}C-{^{1}H} n.m.r. spectrum of the complex [WRh(μ-CMe)(CO)$_3$(η-C_5H_5)(η-C_5Me_5)] the μ-*C*Me resonance occurs at δ 332.8 p.p.m. [*J*(RhC) 27 Hz].[10] Signals are also observed (Table 2) in the spectrum of (4) for three WCO groups and for one CO ligand terminally bound to a rhodium atom [*J*(RhC) 81 Hz]. The latter resonance is broadened due to unresolved ^{31}P–^{13}C coupling.

Despite several attempts, it proved impossible to obtain crystals of (4) for an *X*-ray diffraction study. This was because the complex slowly isomerised in solution, a property which will be discussed later.

If the reaction between [Rh_2(μ-PPh_2)$_2$(cod)$_2$] and [W(≡CMe)(CO)$_2$(η-C_5H_5)] is carried out using an excess of the latter reagent (4:1), a mixture of tungsten–rhodium complexes is obtained. Under these conditions, however, a longer reaction time (*ca.* 3—4 h) is required. Chromatography of the product mixture afforded the complexes [W_2Rh_2(μ-CO){μ-C(Me)C(O)}(μ-PPh_2)$_2$(μ$_3$-CMe)(CO)$_2$(η-C_5H_5)$_2$] (5) and [W_3Rh_2(μ-CO)$_2$(μ-CMe){μ-C(Me)C(O)}(μ-PPh_2)$_2$(μ$_3$-CMe)(CO)$_2$(η-C_5H_5)$_3$] (6). Compound (5) was isolated in two diastereoisomeric forms, which were green (**5a**) and grey (**5b**), and had very similar spectral properties. Data for these new complexes are given in Tables 1—3, but their formulation was not fully established until the structure of (6) had been determined by *X*-ray diffraction. Despite the poor quality of the *X*-ray analysis, caused by decomposition of the crystal in the *X*-ray beam (see Experimental section), the C, O, and P atoms of (6) were unambiguously located.

Selected molecular parameters are listed in Table 4 and the structure is shown in Figure 1. The core of the molecule comprises an essentially planar five-metal-atom chain (mean deviation from plane 0.040 Å) consisting of three tungsten and two rhodium atoms. The metal separations fall into two groups. In the first group are Rh(1)–W(2) [2.791(6) Å] and

Table 1. Analytical[a] and physical data for the complexes

Compound		Colour	Yield (%)	ν(CO)[b]/cm^{-1}		Analysis	
						C	H
(4)	[W$_2$Rh$_2$(μ-CMe)$_2$(μ-PPh$_2$)$_2$(CO)$_4$(η-C$_5$H$_5$)$_2$]	Dark green	79	1 962vs, 1 872m(br),	1 931vs, 1 838m(br)	40.4(40.7)	2.7(2.4)
(5a)[c]	[W$_2$Rh$_2$(μ-CO){μ-C(Me)C(O)}(μ-PPh$_2$)$_2$(μ$_3$-CMe)-(CO)$_2$(η-C$_5$H$_5$)$_2$]	Green	20	2 052s, 1 884vs,	1 995m, 1 746m(br)	[d]37.2(37.4)	2.8(2.6)
(5b)[c]	[W$_2$Rh$_2$(μ-CO){μ-C(Me)C(O)}(μ-PPh$_2$)$_2$(μ$_3$-CMe)-(CO)$_2$(η-C$_5$H$_5$)$_2$]	Grey	16	2 040s, 1 906vs,	1 993m, 1 747m	[d]37.0(37.4)	2.9(2.6)
(6)	[W$_3$Rh$_2$(μ-CO)$_2$(μ-CMe){μ-C(Me)C(O)}(μ-PPh$_2$)$_2$-(μ$_3$-CMe)(CO)$_2$(η-C$_5$H$_5$)$_3$]	Brown	46	1 956s, 1 768m,	1 884vs, 1 743s	[d]36.6(36.4)	2.9(2.6)
(7)	[W$_3$Rh$_2$(μ-CO)$_3$(μ-CMe){μ-C(Me)PPh$_2$}(μ-PPh$_2$)-(μ$_3$-CMe)(CO)$_2$(η-C$_5$H$_5$)$_3$]	Red	80	1 914vs, 1 737m,	1 786m, 1 715m	38.3(38.9)	2.9(2.8)

[a] Calculated values are given in parentheses. [b] Measured in thf. [c] Two isomers, see text. [d] Crystallised with two molecules of CH$_2$Cl$_2$.

Table 2. Hydrogen-1 and carbon-13 n.m.r. data[a] for the tungsten–rhodium complexes

Compound	^{1}H(δ)[b]	^{13}C(δ)[c]
(4)	2.57, 3.48 (s × 2, 6 H, Me), 5.33, 5.45 (s × 2, 10 H, C$_5$H$_5$), 7.10—7.72 (m, 20 H, Ph)	[d]349.1 [d of d, μ-C, *J*(RhC) 37, *J*(PC) 7], 346.5 [d of d, μ-C, *J*(RhC) 29, *J*(PC) 14], 227.4, 218.5, 214.0 (WCO), 199.5 [d, RhCO, *J*(RhC) 81], 148.6—120.9 (Ph), 88.9, 88.5 (C$_5$H$_5$), 50.4, 49.6 (Me)
(5a)[e]	1.59, 2.27, (s × 2, 6 H, Me), 4.92, 5.04 (s × 2, 10 H, C$_5$H$_5$), 6.45—8.00 (m, 20 H, Ph)	301.2 [d of d, μ$_3$-C, *J*(RhC) 19, 10], 253.5 [d, μ-CO, *J*(RhC) 24], 225.5 (WCO), 211.0 [d, μ-C(Me)*C*(O), *J*(PC) 6], 192.5 [d of d, RhCO, *J*(RhC) 67, *J*(PC) 95], 147.5—126.1 (Ph), 118.9 [d, μ-*C*(Me)C(O), *J*(RhC) 18], 90.7, 89.9 (C$_5$H$_5$), 45.3 (μ$_3$-C*Me*), 22.5 [μ-C(*Me*)C(O)]
(5b)[e]	2.56, 3.58 (s × 2, 6 H, Me), 4.91, 5.11 (s × 2, 10 H, C$_5$H$_5$), 6.40—8.00 (m, 20 H, Ph)	305.2 [d of d, μ$_3$-C, *J*(RhC) 20, 10], 258.0 [d, μ-CO, *J*(RhC) 24], 226.8 (WCO), 214.5 [d, μ-C(Me)*C*(O), *J*(PC) 6], 192.4 [d of d, RhCO, *J*(RhC) 70, *J*(PC) 168], 150.5—126.5 (Ph), 100.5 [d, μ-*C*(Me)C(O), *J*(RhC) 31], 91.8, 90.3 (C$_5$H$_5$), 46.0 (μ$_3$-C*Me*), 25.0 [μ-C(*Me*)C(O)]
(6)	1.81, 2.07, 2.59 (s × 3, 9 H, Me), 4.93, 4.99, 5.45 (s × 3, 15 H, C$_5$H$_5$), 7.20—7.62 (m, 20 H, Ph)	361.4 [d, μ-C, *J*(RhC) 32], 312.8 [d of d, μ$_3$-C, *J*(RhC) 29, 20], 258.8 [d, μ-CO, *J*(RhC) 24], 223.6 (WCO), 208.0 [μ-C(Me)*C*(O)], 146.5—127.0 (Ph), 117.0 [d, μ-*C*(Me)C(O), *J*(RhC) 20], 91.6, 90.6, 90.1 (C$_5$H$_5$), 47.0, 42.7 (μ-C*Me*), 28.2 [μ-C(*Me*)C(O)]
(7)	1.79 [d, 3 H, Me, *J*(PH) 16], 2.37, 3.48 (s × 2, 6 H, Me), 5.10, 5.24, 5.28 (s × 3, 15 H, C$_5$H$_5$), 6.95—7.50 (m, 20 H, Ph)	352.1 [d, μ-C, *J*(RhC) 34], 309.0 [d of d, μ$_3$-C, *J*(RhC) 26, 24], 259.1 [d, μ-CO, *J*(RhC) 27], 253.9 [d, μ-CO, *J*(RhC) 37], 245.9 (br, μ-CO), 227.0 (br, WCO), 223.4 [d, WCO, *J*(PC) 34], 147.3—127.5 (Ph), 144.3 [apparent t, μ-*C*(Me)PPh$_2$, *J*(RhC) 37, *J*(PC) 37], 94.4, 92.1, 90.9 (C$_5$H$_5$), 46.5, 31.1 (μ-C*Me*), 22.7 [μ-C(*Me*)PPh$_2$]

[a] Chemical shifts (δ) in p.p.m., coupling constants in Hz. Measurement at room temperature. [b] Measured in CD$_2$Cl$_2$. [c] Hydrogen-1 decoupled, chemical shifts are positive to high frequency of SiMe$_4$. Measurements in CD$_2$Cl$_2$—CH$_2$Cl$_2$ unless otherwise stated. [d] Measured in C$_6$D$_5$CD$_3$. [e] Two isomers, see text.

Table 3. Phosphorus-31 n.m.r. data[a] for the complexes

Compound	^{31}P(δ)[b]
(4)	271.2 [t of d, *J*(RhP) 132, 103; *J*(PP) 132]
	162.2 [d of d, *J*(RhP) 98, *J*(PP) 132]
(5a)[c]	164.7 [d, *J*(RhP) 137]
	159.8 [d, *J*(RhP) 76]
(5b)[c]	173.9 [d of d, *J*(RhP) 98, *J*(PP) 6]
	160.9 [d of d, *J*(RhP) 81, *J*(PP) 6]
(6)	170.1 [d, *J*(RhP) 139]
	147.6 [d, *J*(RhP) 139]
(7)	169.5 [d, PPh$_2$, *J*(RhP) 127]
	−29.6 [s, μ-C(Me)PPh$_2$]

[a] Chemical shifts (δ) in p.p.m., coupling constants in Hz. Measurements in CD$_2$Cl$_2$ at room temperature. [b] Hydrogen-1 decoupled, chemical shifts are positive to high frequency of 85% H$_3$PO$_4$ (external). [c] Two isomers, see text.

Rh(2)–W(3) [2.813(4) Å], distances corresponding to single bonds as found in [WRhH(μ-PPh$_2$)$_2$(CO)$_5$(PPh$_3$)] [2.855(1) Å][11] and [WRh$_2$(acac)$_2$(μ-CO)(μ$_3$-CC$_6$H$_4$Me-4)(CO)$_2$(η-C$_5$H$_5$)] (acac = acetylacetonate) [2.809(2) Å].[12] In the second group are Rh(1)–W(1) [2.696(5) Å] and Rh(2)–W(2) [2.664(5) Å], with separations sufficiently short as to be regarded as Rh=W double bonds. Similarly short rhodium–tungsten distances have been observed in the complex [WRh(μ-CC$_6$H$_4$-Me-4)(CO)$_2$(PPh$_3$)$_2$(η^5-C$_2$B$_9$H$_9$Me$_2$)] [2.681(1) Å][13] and [WRh(μ-CO)$_2$(CO)(PPh$_3$)$_2$(η-C$_5$H$_5$)] [2.587(1) Å],[14] species for which metal–metal double bonding has also been invoked.

As expected, the molecule contains two μ-PPh$_2$ groups, and these bridge the Rh(1)–W(2) and Rh(2)–W(3) linkages. There are also two asymmetrically bridging CO ligands spanning the Rh(1)–W(1) and Rh(2)–W(2) bonds. In order to assign 18-electron valence shells to the tungsten atoms and 16-electron configurations at the rhodium atoms these CO ligands must be regarded as fully bridging. However, the M–C–O angles are appreciably different [W–C–O 162(4) and 165(6), Rh–C–O 115(3) and 110(4)°].

The molecule also contains two alkylidyne ligands, one of which edge bridges the Rh(1)–W(1) bond, while the other caps the Rh(1)W(2)Rh(2) triangle. The Rh(1) ··· Rh(2) separation [3.115(4) Å], however, implies little or no direct metal–metal bonding. An interesting structural feature of the molecule is the presence of a ketenyl ligand[15] bridging the Rh(2)–W(3) bond. The ketenyl group is evidently formed by CO migration to a μ-ethylidyne ligand originally present in complex **(4)**. A similar transfer of a CO group to an alkylidyne ligand to generate

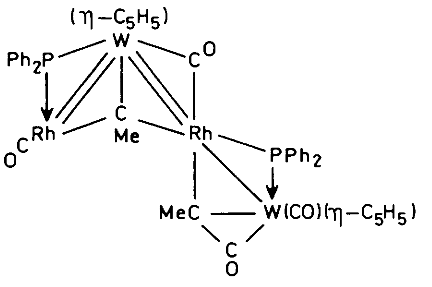

(**5i**)

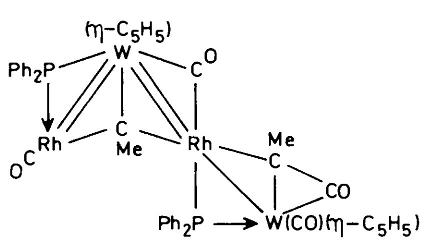

(**5ii**)

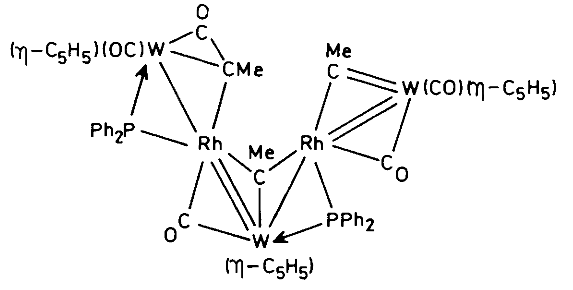

(**6**)

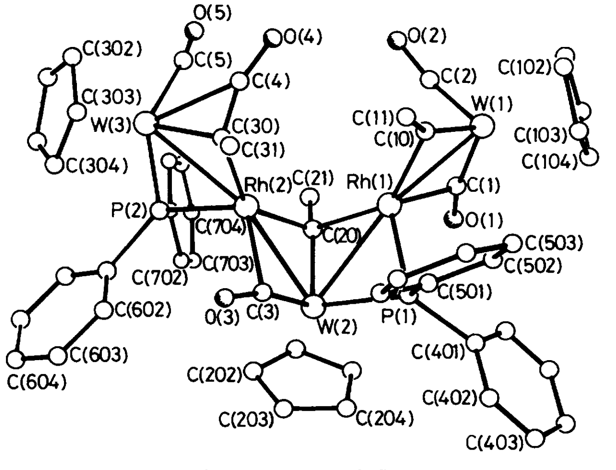

Figure 1. The molecular structure of $[W_3Rh_2(\mu\text{-CO})_2(\mu\text{-CMe})\{\mu\text{-C(Me)C(O)}\}(\mu\text{-PPh}_2)_2(\mu_3\text{-CMe})(CO)_2(\eta\text{-}C_5H_5)_3]$ (**6**) showing the crystallographic numbering

a ketenyl fragment has been observed previously in the formation of the cluster compound $[W_3Ru(\mu\text{-CO})(\mu_3\text{-}\eta\text{-CO})\{\mu\text{-C(Ph)C(O)}\}(\mu\text{-CPh})(\mu_3\text{-CPh})(CO)(PMePh_2)(\eta\text{-}C_5H_5)_3]$.[16] The dimensions of the ketenyl group in the rutheniumtritungsten species are similar to those found in (**6**). In the latter all three tungsten atoms carry a cyclopentadienyl group, and W(1) and W(3) also carry terminal CO ligands.

A striking aspect of the structure of (**6**) is the similarity in conformation with one of the diastereoisomers of the tungsten–platinum chain cluster $[W_3Pt_2(\mu\text{-CC}_6H_4\text{Me-4})_2(\mu_3\text{-CC}_6H_4\text{-Me-4})(CO)_6(\eta\text{-}C_5H_5)_3]$ (**3**).[4a] The arrangement of the metal core atoms in the two species is illustrated in Figure 2. The two complexes are related by virtue of the groups $RhPPh_2$ and PtCO being isoelectronic. However, to obtain 16-electron valence shells at the rhodium atoms in (**6**), as opposed to the formal 14-electron configurations at the platinum atoms in (**3**), two Rh=W bonds are present in the former species, each bridged by a CO ligand.

Having established the structure of (**6**), it was possible to assign the peaks observed in the n.m.r. spectra (Tables 2 and 3). It was evident from the number of resonances observed that in solution only one diastereoisomer was present. In the ^1H n.m.r. spectrum peaks are observed for three Me groups, three C_5H_5 rings, and twenty Ph protons. The $^{13}C\text{-}\{^1H\}$ n.m.r. spectrum shows five resonances above 200 p.p.m., and these may be assigned to the μ-*C*Me, μ_3-*C*Me, μ-CO, CO, and μ-C(Me)*C*(O) groups. The signal at δ 361.4 p.p.m. is characteristic for an alkylidyne carbon edge-bridging a metal–metal bond,[9] and as expected is a doublet due to $^{103}Rh\text{–}^{13}C$ coupling (32 Hz). The triply bridging ethylidyne ligand is responsible for the resonance at δ 312.8 p.p.m. Generally peaks for μ_3-C nuclei occur in the range δ 250—300 p.p.m. depending on the metal atoms involved. However, shifts above 300 p.p.m. are observed for species where the alkylidyne moiety asymmetrically bridges a metal triangle,[9] and there may be such a distortion in (**6**) in solution. The signal at 312.8 p.p.m. shows the expected coupling to two non-equivalent rhodium atoms.

The μ-C(Me)*C*(O) nucleus in complex (**6**) gives rise to a $^{13}C\text{-}\{^1H\}$ n.m.r. resonance at δ 208.0 p.p.m., while the μ-*C*(Me)C(O) carbon of the ketenyl group displays a signal at δ 117.0 p.p.m. The latter may be compared with the resonance at δ 111.9 p.p.m. for the μ-*C*(Ph)C(O) carbon in the spectrum of $[W_3Ru(\mu\text{-CO})(\mu_3\text{-}\eta\text{-CO})\{\mu\text{-C(Ph)C(O)}\}(\mu\text{-CPh})(\mu_3\text{-CPh})(CO)(PMePh_2)(\eta\text{-}C_5H_5)_3]$.[16]

In the CO region there is only one Rh(μ-CO)W resonance [δ 258.8 p.p.m., *J*(RhC) 24 Hz] and one WCO signal (δ 223.6 p.p.m.), where two of each type might have been expected. Since both resonances appeared to correspond in intensity to one carbon nucleus, it is possible that the two missing signals are not seen as a result of dynamic behaviour. This might involve rotation of the $W(1)(CO)_2(\eta\text{-}C_5H_5)$ fragment at the end of the chain (see Figure 1). If coalescence of the peaks occurs at room temperature the signals for C(1)–O(1) and C(2)–O(2) would not be seen. Evidence in support of this idea is given later. In the $^{31}P\text{-}\{^1H\}$ n.m.r. spectrum of (**6**) resonances for the μ-PPh$_2$ ligands occur at δ 147.6 and 170.1 p.p.m. Both signals are doublets, as expected for Rh(μ-PPh$_2$)W fragments.

As mentioned above, two diastereoisomers of (**5**) are formed in the reaction which yields compound (**6**). Although the two isomers could be separated by column chromatography, in solution they slowly interconvert. Consequently it was not possible to obtain $^{13}C\text{-}\{^1H\}$ n.m.r. spectra for (**5a**) and (**5b**) in which resonances for the other species were absent. Nevertheless, unambiguous assignment of peaks to one or other isomer could be made on the basis of the relative intensity of signals measured on samples initially containing a single isomer. There was, however, no difficulty in obtaining ^1H and $^{31}P\text{-}\{^1H\}$ n.m.r. spectra of pure (**5a**) or pure (**5b**) since the accumulation times required for ^1H and ^{31}P nuclei were much faster than the rate at which the equilibrium (5:4) is established.

Assignment of the resonances observed in the n.m.r. spectra of the two diastereoisomers of (**5**) was also aided by the observation that these species were precursors to (**6**). As

Table 4. Selected interatomic distances (Å) and angles (°) for the complexes [$W_3Rh_2(\mu\text{-}CO)_2(\mu\text{-}CMe)\{\mu\text{-}C(Me)C(O)\}(\mu\text{-}PPh_2)_2(\mu_3\text{-}CMe)(CO)_2(\eta\text{-}C_5H_5)_3$] (**6**) and [$W_3Rh_2(\mu\text{-}CO)_3(\mu\text{-}CMe)\{\mu\text{-}C(Me)PPh_2\}(\mu\text{-}PPh_2)(\mu_3\text{-}CMe)(CO)_2(\eta\text{-}C_5H_5)_3$] (**7**)

	(6)	(7)		**(6)**	(7)		**(6)**	(7)
W(1)–Rh(1)	2.696(5)	2.678(2)	W(2)–Rh(1)	2.791(6)	2.803(2)	W(2)–Rh(2)	2.664(5)	2.699(2)
W(3)–Rh(2)	2.813(4)	2.786(2)	Rh(1) • • • Rh(2)	3.115(4)	3.049(2)	W(2)–P(1)	2.36(1)	2.330(6)
Rh(1)–P(1)	2.24(2)	2.263(6)	W(3)–P(2)	2.36(2)	2.382(6)	Rh(2)–P(2)	2.28(1)	—
W(1)–C(1)	1.88(7)	1.96(2)	Rh(1)–C(1)	2.18(6)	2.23(2)	W(1)–C(2)	1.75(5)	1.97(3)
W(1)–C(10)	1.80(5)	1.85(2)	Rh(1)–C(10)	2.04(5)	1.99(2)	W(2)–C(3)	1.90(7)	1.98(2)
Rh(2)–C(3)	2.19(6)	2.16(2)	W(2)–C(20)	1.90(6)	1.97(2)	Rh(1)–C(20)	2.01(5)	2.03(2)
Rh(2)–C(20)	1.95(6)	2.04(2)	W(3)–C(4)	2.27(5)	2.01(2)	Rh(2)–C(4)	—	2.06(2)
W(3)–C(5)	2.15(11)	1.95(3)	W(3)–C(30)	2.03(4)	2.12(2)	Rh(2)–C(30)	2.03(7)	2.03(2)
P(2)–C(30)	—	1.73(2)	C(4)–C(30)	1.39(9)	—	C(1)–O(1)	1.31(9)	1.20(2)
C(2)–O(2)	1.28(7)	1.14(3)	C(3)–O(3)	1.19(8)	1.16(2)	C(4)–O(4)	1.19(8)	1.21(2)
C(5)–O(5)	1.0(1)	1.16(3)						
W(1)–Rh(1)–W(2)	165.6(2)	158.9(1)	W(2)–Rh(2)–W(3)	163.6(2)	149.3(1)	Rh(1)–W(2)–Rh(2)	69.6(1)	67.3(1)
W(1)–Rh(1)–P(1)	117.8(3)	122.2(2)	W(2)–Rh(2)–P(2)	112.2(5)	—	Rh(1)–P(1)–W(2)	74.8(4)	75.2(2)
Rh(2)–P(2)–W(3)	74.7(6)	—	Rh(2)–W(3)–P(2)	76.9(1)	—	Rh(1)–W(1)–C(1)	53(2)	54.9(7)
Rh(1)–W(1)–C(2)	88(2)	90.2(7)	W(1)–Rh(1)–C(1)	44(2)	46.0(6)	W(1)–C(10)–Rh(1)	89(2)	88.3(7)
W(2)–C(3)–Rh(2)	81(3)	81.3(7)	W(2)–C(20)–Rh(1)	91(2)	89(8)	W(2)–C(20)–Rh(2)	88(3)	84.7(8)
Rh(1)–C(20)–Rh(2)	104(3)	97.3(9)	P(1)–W(2)–C(3)	92(2)	94.6(6)	W(3)–P(2)–C(30)	—	59.4(7)
W(2)–Rh(2)–C(3)	45(2)	46.6(5)	Rh(2)–W(2)–C(3)	54(2)	52.1(5)	W(3)–Rh(2)–C(30)	46(1)	49.1(6)
W(3)–C(30)–Rh(2)	88(3)	84.3(7)	W(3)–Rh(2)–C(4)	—	46.2(6)	Rh(2)–W(3)–C(5)	98(2)	104.9(7)
W(1)–C(1)–O(1)	162(4)	164(2)	W(1)–C(2)–O(2)	171(7)	178(2)	Rh(1)–C(1)–O(1)	115(4)	117(2)
W(1)–C(10)–C(11)	149(4)	147.2(6)	Rh(1)–C(10)–C(11)	119(4)	124(1)	W(2)–C(3)–O(3)	165(6)	166(2)
Rh(2)–C(3)–O(3)	110(4)	118(1)	Rh(2)–C(20)–Rh(1)	115(3)	122(1)	W(2)–C(20)–C(21)	143(5)	136(2)
Rh(1)–C(20)–C(21)	109(3)	118(1)	W(3)–C(4)–O(4)	145(4)	151(2)	W(3)–C(4)–C(30)	62(3)	—
Rh(2)–C(30)–C(4)	109(5)	—	Rh(2)–C(4)–O(4)	—	123(2)	W(3)–C(5)–O(5)	173(5)	175(2)
W(3)–C(30)–C(31)	132(3)	130(1)	Rh(2)–C(30)–C(31)	121(4)	117(1)	Rh(2)–C(30)–P(2)	—	118(1)
P(2)–C(30)–C(31)	—	121(2)	C(4)–C(30)–C(31)	118(6)	—	C(30)–C(4)–O(4)	153(5)	—

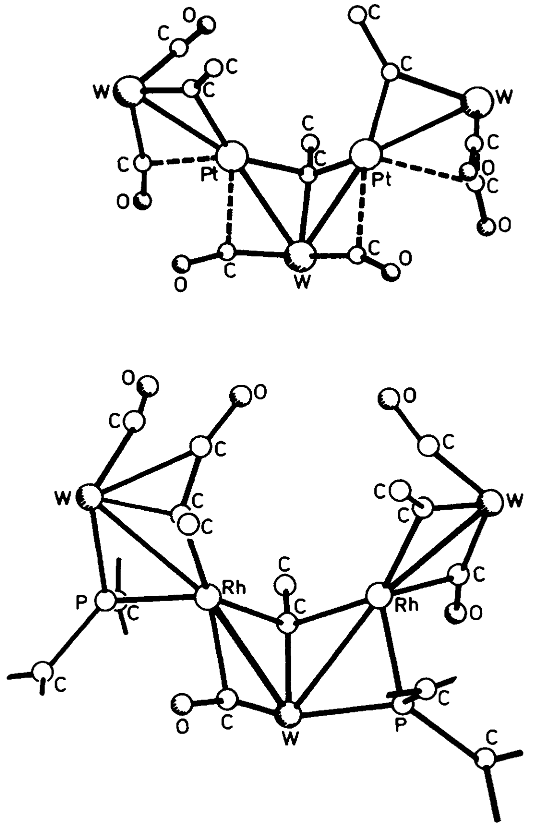

Figure 2. Arrangement of the metal atom cores in the molecules (**3**) and (**6**)

discussed above, the n.m.r. data for the latter were in accord with the structure established by *X*-ray diffraction. Because the spectra of (**5a**) and (**5b**) were very similar, only data for the former will be discussed.

The ^1H n.m.r. spectrum of (**5a**) had resonances for two C_5H_5 and two Me groups, while the $^{13}C\text{-}\{^1H\}$ n.m.r. spectrum revealed diagnostic signals for μ_3-CMe, Rh(μ-CO)W, WCO, and RhCO groups, together with peaks for the μ-C(Me)C(O) ligand (Table 2). The resonance at δ 301.2 p.p.m., with two $^{103}Rh\text{–}^{13}C$ couplings, clearly arises from the ligating carbon of an ethylidyne group capping a WRh_2 triangle in which the two rhodium atoms are not equivalent. The doublet [*J*(RhC) 24 Hz] at 253.5 p.p.m. is evidently due to a Rh(μ-CO)W group, and the peak at 225.5 may be assigned to a CO ligand terminally bound to tungsten. There is also a diagnostic resonance for a RhCO group at δ 192.5 p.p.m. This resonance appears as a doublet of doublets [*J*(RhC) 67, *J*(PC) 95 Hz]. Assignment of $^{103}Rh\text{–}^{13}CO$ and $Ph_2{}^{31}P\text{–}^{13}CO$ couplings in the $^{13}C\text{-}\{^1H\}$ n.m.r. spectra of the compounds reported herein is made on the basis of the former occurring in the range 60—80 Hz, whereas the latter vary appreciably with the geometry about the rhodium atom. The value of 95 Hz for the $^{31}P\text{–}^{13}C$ coupling is consistent with a transoid–Ph_2PRhCO arrangement in (**5a**).

The chemical shifts for the ligating carbons of the μ-*C*(Me)*C*(O) moiety (δ 211.0 and 118.9 p.p.m., respectively) are very similar to those for the corresponding peaks in the spectrum of (**6**) (δ 208.0 and 117.0 p.p.m.). The $^{31}P\text{-}\{^1H\}$ n.m.r. data for (**5a**) (Table 3) reveal the presence of two μ-PPh_2 ligands.

It was thus evident from the n.m.r data that the tetranuclear metal species (**5a**) [or (**5b**)] has structural features in common with those of the pentanuclear metal cluster (**6**). We therefore assign the structures shown [(**5i**) and (**5ii**)] to the two isomers of (**5**). However, our inability to carry out an *X*-ray diffraction study on either of the species (**5a**) and (**5b**) means that a specific

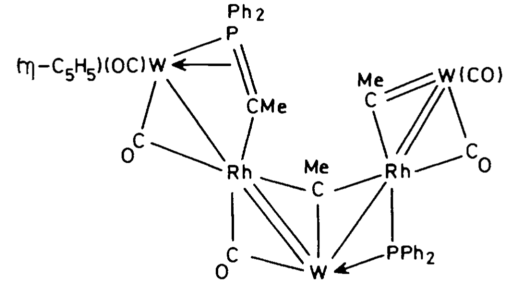

(**7**)

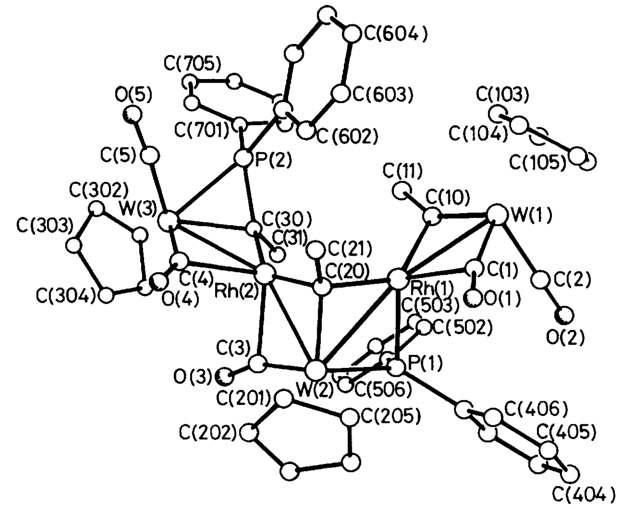

Figure 3. The molecular structure of $[W_3Rh_2(\mu\text{-}CO)_3(\mu\text{-}CMe)\{\mu\text{-}C(Me)PPh_2\}(\mu\text{-}PPh_2)(\mu_3\text{-}CMe)(CO)_2(\eta\text{-}C_5H_5)_3]$ (**7**), showing the crystallographic numbering

structural assignment of these diastereoisomers to one or other of the conformers (**5i**) or (**5ii**) cannot be made.

Diastereoisomerism of the kind depicted for (**5**) has been observed previously in other metal chain clusters.[4a,b] The observed slow interconversion between (**5i**) and (**5ii**) might involve rotation of two halves of the molecule about the central rhodium atom, although other pathways are possible. The difference between the two conformers can be related to the different distances between the terminal rhodium atom and the μ-ketenyl group. If the isomeric mixture of (**5**) remains in solution for periods exceeding 12 h other complexes are formed, as discussed in the following paper.

Having established the structures of the compounds (**5**) and (**6**) it was important to determine how these products related to (**4**), the species isolated when a stoicheiometric amount of the reactants was used. It was found that, over a period of about 2 h in thf solution, compound (**4**) underwent a *ca.* 50% conversion into (**5a**) and (**5b**). It is possible that a reduction in steric crowding is the driving force for this isomerisation. The phosphido group bridging the Rh–Rh bond in (**4**) migrates to bridge the bond between rhodium and the terminal tungsten atom in (**5**). This is accompanied by one of the terminal CO ligands on tungsten migrating to an ethylidyne group to form the μ-C(Me)C(O) fragment. As mentioned above, a related transformation occurs in the formation of $[W_3Ru(\mu\text{-}CO)(\mu_3\text{-}\eta\text{-}CO)\{\mu\text{-}C(Ph)C(O)\}(\mu\text{-}CPh)(\mu_3\text{-}CPh)(CO)(PMePh_2)(\eta\text{-}C_5H_5)_3]$ upon treatment of $[W_3Ru(\mu\text{-}CO)(\mu_3\text{-}\eta\text{-}CO)(\mu\text{-}CPh)_2(\mu_3\text{-}CPh)(CO)_2(\eta\text{-}C_5H_5)_3]$ with $PMePh_2$.[16]

Once compound (**4**) is transformed into (**5**), the pentanuclear metal complex (**6**) can form if a molecule of $[W(\equiv CMe)(CO)_2(\eta\text{-}C_5H_5)]$ displaces the CO group attached to the rhodium at the end of the chain in (**5**). It is interesting that whereas compound (**5**) exists as two conformers it gives rise to (**6**) as a single diastereoisomer. One possible explanation for this observation is that in (**5ii**) attack at the RhCO group may be impeded by the proximity of the μ-PPh_2 ligand at the other end of the chain. Consequently, (**5i**) might react preferentially with $[W(\equiv CMe)(CO)_2(\eta\text{-}C_5H_5)]$ to generate the observed configuration of (**6**). Removal of (**5i**) in this manner will shift the equilibrium involving (**5ii**) so that eventually both diastereoisomers of (**5**) are consumed. In contrast with (**6**), the platinum–tungsten cluster (**3**) exists in solution in more than one diastereomeric form.[4a] It is assumed that preference for one or other of the various possible diastereoisomers involving the chain structures[4b] is influenced by the steric requirements of the bridging ligands supporting the metal–metal bonds. The bulky PPh_2 groups present in the compounds described herein might well lead to fewer diastereoisomers existing in solution compared with other systems.[4]

Initial attempts to grow crystals of complex (**6**) for the *X*-ray diffraction study described above were carried out at room temperature. During the period required it was observed that (**6**) was quantitatively converted into a new red complex (**7**). An *X*-ray diffraction study identified (**7**) as $[W_3Rh_2(\mu\text{-}CO)_3(\mu\text{-}CMe)\{\mu\text{-}C(Me)PPh_2\}(\mu\text{-}PPh_2)(\mu_3\text{-}CMe)(CO)_2(\eta\text{-}C_5H_5)_3]$ (Table 4 and Figure 3).

The metal framework of complex (**7**) is very similar to that of (**6**). Again there is an almost coplanar chain of metal atoms. Moreover, as with (**6**), the Rh(1)–W(1) [2.678(2) Å] and Rh(2)–W(2) [2.699(2) Å] bonds in (**7**) are significantly shorter than the Rh(1)–W(2) [2.803(2) Å] and Rh(2)–W(3) [2.786(2) Å] linkages. This is consistent with the two shorter metal–metal distances corresponding to Rh=W bonds. There are five CO ligands, three of which bridge metal–metal bonds. This feature is also revealed in the i.r. spectrum (Table 1) with the observation of bands at 1 786, 1 737, and 1 715 cm^{-1}.

The most significant difference between the structures of (**6**) and (**7**) is that the CO group in the μ-C(Me)C(O) fragment of (**6**) has exchanged positions with the μ-PPh_2 ligand bridging the Rh(2)–W(3) bond. Consequently, in (**7**) the Rh(2)–W(3) vector is now spanned by a CO ligand and a μ-C(Me)PPh_2 moiety. The latter may be regarded as a bridging λ^5-phospha-alkyne ($MeC\equiv PPh_2$). Recently this type of ligand has been structurally identified ligating a single metal centre in the complexes $[Ta(H)_2(PMe_3)(\eta^2\text{-}CHPMe_2)(\eta\text{-}C_5Me_5)]$[17] and $[Ta(PMe_3)_3(\eta^2\text{-}CH_2PMe_2)(\eta^2\text{-}CHPMe_2)]$.[18] However, (**7**) appears to be the first example of a compound in which a λ^5-phospha-alkyne ligand bridges two metal centres. The ligand is formed by a coupling of a μ-PPh_2 group with an ethylidyne ligand to generate a new C–P bond. Relevant to this result is the coupling of a μ-PPh_2 group and a methoxymethylene ligand in the synthesis of $[WOs(\mu\text{-}PPh_2)\{\mu\text{-}\sigma,\sigma'\text{-}CH(OMe)PPh_2\}(CO)_6(PMePh_2)]$,[19] and the linking of $\mu_3\text{-}PC_6H_4OMe\text{-}4$ and CH_2 groups in the formation of the complex $[Fe_3\{\mu\text{-}\sigma,\sigma'\text{:}\eta^2\text{-}P(C_6H_4OMe\text{-}4)CH_2\}(\mu\text{-}CO)(CO)_9]$.[20] The latter contains a phospha-alkene fragment in which the carbon–phosphorus distance [1.76(1) Å] is comparable with the C(30)–P(2) separation [1.73(2) Å] in (**7**). Both distances are considerably shorter than that expected for a C–P single bond (1.825 Å),[21] and are close to the separations (1.68—1.72 Å) associated with C=P linkages in free phospha-alkenes.[22]

Although the mechanism for the conversion of complex (**6**) into (**7**) is not known, it is possible that the isomerisation proceeds *via* an intermediate in which a λ^5-phospha-alkyne fragment transversely bridges the Rh(2)–W(3) vector (Figures 1 and 2). Thus formation of a μ-C(Me)PPh_2 unit might accompany migration of the CO group of the ketenyl ligand to a terminal site on the tungsten centre. Such an intermediate might then be converted into (**7**) by cleavage of the P(2)–Rh(2) bond and concomitant migration of one of the terminal CO ligands in the $W(CO)_2(\eta-C_5H_5)$ fragment into a bridging site across the Rh(2)–W(3) vector. It may be noted that compounds with λ^3-phospha-alkynes bridging a dimetal centre have been reported,[23] and a λ^5-phospha-alkyne could adopt a similar bonding mode.

The n.m.r. data for complex (**7**) (Tables 2 and 3) agree well with the structure established by *X*-ray diffraction. In the $^{31}P-\{^1H\}$ n.m.r. spectrum there is a high field signal at δ −29.6 p.p.m. which may be ascribed to the μ-C(Me)*P*Ph_2 nucleus.[17,18] Another resonance, a doublet at δ 169.5 p.p.m. [*J*(RhP) 127 Hz], is characteristic for the μ-PPh_2 ligand present in (**7**). In the ^1H n.m.r. spectrum the signal for the methyl group in the μ-C(Me)PPh_2 ligand occurs as a doublet (16 Hz) due to $^{31}P-^1H$ coupling. The $^{13}C-\{^1H\}$ n.m.r. spectrum shows all the expected peaks. There are two features of special interest. A resonance at δ 144.3 p.p.m. is assigned to the μ-*C*(Me)PPh_2 nucleus. This signal shows coupling both to ^{31}P and ^{103}Rh. In the CO region of the spectrum there are five resonances as expected. However, the peaks at δ 245.9 and 227.0 p.p.m. are broad indicating dynamic behaviour. We ascribe these resonances to the C(1)O(1) and C(2)O(2) ligands (Figure 3). Reference was made earlier to the absence in the $^{13}C-\{^1H\}$ n.m.r. spectrum of (**6**) of peaks due to the corresponding CO groups, and this was attributed to site exchange of these ligands. Evidently for (**7**) the process requires a higher activation energy since two signals are seen, albeit broad bands.

The work described herein has shown how novel chain-type tungsten–rhodium complexes can be prepared in which the metal–metal bonds are bridged by CMe, PPh_2, C(Me)C(O), or C(Me)PPh_2 fragments. We have also demonstrated the formation of a μ-λ^5-phospha-alkyne by coupling of ethylidyne and phosphido ligands.

Experimental

The techniques and equipment used have been described previously.[1] Light petroleum refers to that fraction of b.p. 40—60 °C. All experiments were carried out using Schlenk-tube techniques, under oxygen-free nitrogen. Alumina (Brockman Activity II) was used for chromatography columns (3 × 25 cm). Analytical and other data for the new compounds are given in Table 1. The reagents $[W(\equiv CMe)(CO)_2(\eta-C_5H_5)]$[24] and $[Rh_2(\mu-PPh_2)_2(cod)_2]$[5] were prepared by methods previously reported.

Reactions between $[Rh_2(\mu-PPh_2)_2(cod)_2]$ *and* $[W(\equiv CMe)(CO)_2(\eta-C_5H_5)]$.—(*i*) A thf (25 cm^3) solution of $[Rh_2(\mu-PPh_2)_2(cod)_2]$ (0.20 g, 0.25 mmol) was treated with $[W(\equiv CMe)(CO)_2(\eta-C_5H_5)]$ (0.17 g, 0.51 mmol), and the mixture was stirred for 10 min. Solvent was removed *in vacuo*, and the green-brown residue was dissolved in CH_2Cl_2–light petroleum (10 cm^3, 1:1) and chromatographed. Elution with the same solvent mixture afforded a green-brown eluate. Solvent was removed *in vacuo* and the residue was crystallised at *ca.* −10 °C from CH_2Cl_2–

Table 5. Atomic positional parameters (fractional co-ordinates × 10^4) for complex (**6**), with standard deviations in parentheses

Atom	*x*	*y*	*z*
W(1)	14 888(3)	12 254(2)	4 817(1)
W(2)	13 097(3)	11 386(2)	2 353(1)
W(3)	9 113(3)	6 087(2)	1 401(1)
Rh(1)	13 842(5)	11 499(3)	3 537(2)
Rh(2)	11 366(5)	8 906(3)	2 073(2)
P(1)	15 636(15)	12 715(11)	3 331(6)
P(2)	8 820(17)	7 453(12)	1 152(7)
C(1)	13 992(57)	12 781(40)	4 385(23)
O(1)	13 457(40)	13 361(28)	4 271(16)
C(2)	12 929(65)	10 857(46)	4 522(25)
O(2)	11 616(55)	9 804(39)	4 368(21)
C(3)	13 213(57)	10 081(41)	1 903(23)
O(3)	13 286(43)	9 364(31)	1 524(17)
C(4)	10 958(62)	7 208(43)	2 500(24)
O(4)	11 151(46)	7 302(32)	3 011(18)
C(5)	8 145(92)	6 024(66)	2 022(37)
O(5)	7 615(61)	5 873(43)	2 262(25)
C(10)	14 741(45)	11 090(31)	4 153(18)
C(11)	15 293(58)	10 342(44)	3 934(24)
C(20)	11 843(56)	10 540(39)	2 667(22)
C(21)	10 438(55)	10 296(42)	2 803(24)
C(30)	11 507(58)	7 544(41)	2 109(23)
C(31)	12 945(54)	7 655(40)	2 153(23)
C(101)	15 888(50)	12 893(99)	5 947(21)
C(102)	16 823	12 686	5 746
C(103)	17 680	13 668	5 625
C(104)	17 274	14 481	5 750
C(105)	16 167	14 002	5 949
C(201)	11 677(39)	11 930(33)	1 992(18)
C(202)	11 743	11 248	1 455
C(203)	13 361	12 095	1 629
C(204)	14 294	13 300	2 274
C(205)	13 253	13 197	2 498
C(301)	6 988(44)	3 771(36)	601(22)
C(302)	8 400	4 011	970
C(303)	9 545	4 733	828
C(304)	8 850	4 939	371
C(305)	7 275	4 344	231
C(402)	18 146(36)	15 234(25)	3 707(14)
C(403)	19 108	16 623	4 017
C(404)	18 861	17 332	4 438
C(405)	17 653	16 654	4 549
C(406)	16 692	15 266	4 239
C(401)	16 939	14 556	3 818
C(502)	18 287(39)	13 239(26)	4 171(13)
C(503)	19 406	13 084	4 334
C(504)	19 345	12 219	3 825
C(505)	18 165	11 510	3 154
C(506)	17 046	11 665	2 991
C(501)	17 107	12 259	3 500
C(602)	9 724(28)	7 581(25)	232(14)
C(603)	9 400	7 280	−405
C(604)	7 859	6 616	−914
C(605)	6 642	6 254	−787
C(606)	6 965	6 554	−150
C(601)	8 506	7 218	359
C(702)	7 607(36)	9 723(29)	1 109(15)
C(703)	6 707	9 070	1 202
C(704)	5 677	8 463	1 401
C(705)	5 548	7 510	1 507
C(706)	6 449	7 163	1 413
C(701)	7 478	7 770	1 215
C(01)*	17 357(77)	18 098(52)	3 266(30)
Cl(1)*	15 325(25)	16 480(15)	2 774(9)
Cl(2)*	17 839(29)	19 252(18)	3 881(13)
C(02)*	9 457(72)	4 190(55)	2 570(31)
Cl(3)*	7 445(29)	2 892(22)	2 004(11)
Cl(4)*	10 614(38)	3 950(33)	2 275(13)

* Solvent molecule.

Table 6. Atomic positional parameters (fractional co-ordinates × 10^4) for complex (**7**), with standard deviations in parentheses

Atom	*x*	*y*	*z*
W(1)	910(1)	−33(1)	3 552(1)
W(2)	3 065(1)	1 509(1)	3 377(1)
W(3)	3 106(1)	1 360(1)	956(1)
Rh(1)	1 892(1)	768(1)	3 250(1)
Rh(2)	2 792(1)	1 230(1)	2 197(1)
P(1)	1 906(3)	1 699(3)	3 650(3)
P(2)	2 043(3)	803(3)	944(2)
C(10)	992(10)	478(8)	2 892(8)
C(11)	712(12)	669(11)	2 271(9)
C(20)	2 904(11)	736(10)	2 974(9)
C(21)	3 270(11)	124(9)	2 970(10)
C(30)	2 160(10)	1 379(9)	1 462(9)
C(31)	1 598(12)	1 887(10)	1 530(10)
C(1)	1 816(12)	59(10)	3 964(10)
O(1)	2 308(8)	−3(7)	4 300(7)
C(2)	498(13)	535(12)	4 136(11)
O(2)	239(9)	857(8)	4 470(7)
C(3)	3 053(10)	2 050(8)	2 657(8)
O(3)	3 153(8)	2 468(7)	2 359(7)
C(4)	3 700(11)	1 157(10)	1 690(9)
O(4)	4 263(8)	1 049(7)	1 919(7)
C(5)	3 426(12)	577(11)	695(10)
O(5)	3 646(10)	129(9)	509(8)
C(101)	−40(10)	−669(9)	3 826(8)
C(102)	−64	−532	3 190
C(103)	542	−778	2 910
C(104)	941	−1 067	3 373
C(105)	581	−1 000	3 938
C(201)	4 127(8)	1 118(6)	3 724(7)
C(202)	4 254	1 715	3 538
C(203)	3 863	2 098	3 927
C(204)	3 494	1 738	4 354
C(205)	3 657	1 132	4 229
C(301)	2 757(7)	2 152(8)	336(8)
C(302)	3 292	1 828	28
C(303)	3 922	1 894	368
C(304)	3 777	2 258	885
C(305)	3 057	2 418	865
C(402)	1 073(7)	2 193(6)	4 610(6)
C(403)	840	2 220	5 216
C(404)	1 097	1 818	5 649
C(405)	1 587	1 388	5 476
C(406)	1 820	1 360	4 870
C(401)	1 563	1 763	4 437
C(502)	597(7)	2 031(5)	3 158(6)
C(503)	149	2 400	2 824
C(504)	400	2 929	2 571
C(505)	1 100	3 090	2 651
C(506)	1 549	2 721	2 985
C(501)	1 297	2 192	3 238
C(602)	2 213(7)	−162(7)	1 729(7)
C(603)	2 117	−748	1 928
C(604)	1 727	−1 145	1 573
C(605)	1 435	−957	1 019
C(606)	1 531	−372	821
C(601)	1 920	26	1 176
C(702)	716(9)	1 005(8)	452(6)
C(703)	249	1 131	−23
C(704)	493	1 182	−624
C(705)	1 204	1 108	−750
C(706)	1 671	983	−275
C(701)	1 427	931	326

light petroleum (10 cm^3, 1:3) to give dark green *microcrystals* of [W$_2$Rh$_2$(μ-CMe)$_2$(μ-PPh$_2$)$_2$(CO)$_4$(η-C$_5$H$_5$)$_2$] (**4**) (0.25 g).

(*ii*) A mixture of the compounds [Rh$_2$(μ-PPh$_2$)$_2$(cod)$_2$] (0.20 g, 0.25 mmol) and [W(≡CMe)(CO)$_2$(η-C$_5$H$_5$)] (0.33 g, 1.0 mmol) was stirred in thf (25 cm^3) for 2 h. During this period the colour of the mixture changed from green to dark brown. Solvent was removed *in vacuo*, and the residue was dissolved in CH$_2$Cl$_2$ (15 cm^3) and chromatographed. Elution with the same solvent removed initially unreacted [W(≡CMe)(CO)$_2$(η-C$_5$H$_5$)] followed by a dark brown fraction, and then a lime-green eluate. Elution with CH$_2$Cl$_2$–thf (10:1) gave a grey eluate. The last three fractions were collected individually, and solvent was removed *in vacuo* from each eluate. The brown residue was crystallised from CH$_2$Cl$_2$–light petroleum (5 cm^3, 1:4) thereby affording brown *crystals* of [W$_3$Rh$_2$(μ-CO)$_2$(μ-CMe){μ-C(Me)C(O)}(μ-PPh$_2$)$_2$(μ$_3$-CMe)(CO)$_2$(η-C$_5$H$_5$)$_3$] (**6**) (0.18 g). Similar treatment of the other two residues gave lime-green *crystals* of [W$_2$Rh$_2$(μ-CO){μ-C(Me)C(O)}(μ-PPh$_2$)$_2$(μ$_3$-CMe)(CO)$_2$(η-C$_5$H$_5$)$_2$] (**5a**) (0.06 g) and grey-black *crystals* of [W$_2$Rh$_2$(μ-CO){μ-C(Me)C(O)}(μ-PPh$_2$)$_2$(μ$_3$-CMe)(CO)$_2$(η-C$_5$H$_5$)$_2$] (**5b**) (0.05 g).

Isomerisation of [W$_3$Rh$_2$(μ-CO)$_2$(μ-CMe){μ-C(Me)C(O)}(μ-PPh$_2$)$_2$(μ$_3$-CMe)(CO)$_2$(η-C$_5$H$_5$)$_3$].—A thf (25 cm^3) solution of complex (**6**) (0.20 g, 0.13 mmol) was stirred at room temperature for 16 h. During this period the solution changed colour from dark brown to red. Solvent was removed *in vacuo*, and the residue was dissolved in CH$_2$Cl$_2$ (10 cm^3) and chromatographed. Elution with the same solvent yielded a red fraction. After removal of solvent *in vacuo*, the residue was crystallised at *ca.* −10 °C from CH$_2$Cl$_2$–light petroleum (10 cm^3, 1:4) giving dark red *crystals* of [W$_3$Rh$_2$(μ-CO)$_3$(μ-CMe){μ-C(Me)PPh$_2$}(μ-PPh$_2$)(μ$_3$-CMe)(CO)$_2$(η-C$_5$H$_5$)$_3$] (**7**) (0.16 g).

Crystal Structure Determinations.—Crystals of complexes (**6**) and (**7**) grow as dark brown and dark red prisms, respectively, from CH$_2$Cl$_2$–light petroleum. Complex (**6**) crystallised with two molecules of CH$_2$Cl$_2$ per asymmetric unit. Crystals of suitable dimensions [*ca.* 0.15 × 0.20 × 0.40 mm for (**6**), and *ca.* 0.30 × 0.40 × 0.80 mm for (**7**)] were sealed in Lindemann tubes under nitrogen. Diffracted intensities were measured (θ–2θ scans) at 298 K in the range $2.9 \leqslant 2\theta \leqslant 50°$ on a Nicolet *P3m* four-circle diffractometer. Of 8 025 unique reflections for (**6**), 3 283 had $F \geqslant 8\sigma(F)$ and of 7 206 unique reflections for (**7**), 3 792 had $F \geqslant 6\sigma(F)$. Only these data were used in the solution and refinement of the structures, after correction for Lorentz, polarisation and *X*-ray absorption effects. The latter correction was based on a semi-empirical method using azimuthal scan data.[25]

Crystal data for (**6**). C$_{50}$H$_{44}$O$_5$P$_2$Rh$_2$W$_3$·2CH$_2$Cl$_2$, M = 1 714.1, triclinic, a = 11.523(2), b = 14.066(5), c = 25.144(9) Å, α = 109.54(3), β = 105.46(2), γ = 121.99(2)°, U = 2 764(1) Å^3, Z = 2, D_c = 2.06 g cm^{-3}, $F(000)$ = 1 620, space group $P\bar{1}$ (no. 2), Mo-K_α X-radiation (graphite monochromator), $\bar{\lambda}$ = 0.710 69 Å, μ(Mo-K_α) = 72.16 cm^{-1}.

Crystal data for (**7**). C$_{50}$H$_{44}$O$_5$P$_2$Rh$_2$W$_3$, M = 1 543.6, orthorhombic, a = 19.091(5), b = 22.245(5), c = 21.804(5) Å, U = 9 335(2) Å^3, Z = 8, D_c = 2.18 g cm^{-3}, $F(000)$ = 5 806, space group *Pbca* (no. 61), μ(Mo-K_α) 83.22 cm^{-1}.

The molecular structure of complex (**6**) was solved by the usual heavy-atom and Fourier difference-methods, while that of (**7**) was solved by direct methods. For (**7**) only the metal and phosphorus atoms were initially located; the light atoms being subsequently located from Fourier-difference methods.

Refinements by blocked-cascade least squares, with anisotropic thermal parameters for all non-hydrogen atoms, were carried out on a Data General S230 'Eclipse' computer for (**6**), and on a DEC microvax II computer for (**7**).[25] The cyclopentadienyl and phenyl rings were constrained to rigid idealised geometries. Aromatic and methyl hydrogen atoms were included in calculated positions (C–H 0.960 Å) with fixed isotropic thermal parameters 1.2 times $U_{\text{equiv.}}$ of their parent carbon atoms. Refinements with the weighting scheme $w^{-1} = [\sigma^2(F_o) + g|F_o|^2]$ [with $g = 0.001\,3$ for (**6**), and 0.000 6 for (**7**)] converged at $R = 0.106$ (R' 0.105) for (**6**), and at $R = 0.051$ (R' 0.049) for (**7**). The final electron-density maps showed no residual peaks $\geqslant 3.3$ or $\leqslant -4.6$ e Å^{-3} for (**6**) and $\geqslant 1.2$ or $\leqslant -1.7$ e Å^{-3} for (**7**) close to the tungsten atoms. The high residuals for (**6**) reflect the relative poor quality of the data resulting from crystal degeneration (40% in 10 d) in the *X*-ray beam. Corrections were applied during the data processing[25] for (**6**) to adjust for decayed intensities, by using standard 'check' reflections, acquired during data collection. Scattering factors and corrections for anomalous dispersion were taken from ref. 26. The atom co-ordinates for (**6**) and (**7**) are given in Tables 5 and 6, respectively.

Additional material available from the Cambridge Crystallographic Data Centre comprises thermal parameters, H-atom co-ordinates, and remaining bond lengths and angles.

Acknowledgements

We thank the S.E.R.C. for research studentships (to S. J. D. and M. U. P.) and the U.S.A.F. Office of Scientific Research for partial support (Grant 86-0125).

References

1 Part 88, J. C. Jeffery, M. A. Ruiz, P. Sherwood, and F. G. A. Stone, *J. Chem. Soc., Dalton Trans.*, preceding paper.
2 B. F. G. Johnson (ed.), 'Transition Metal Clusters,' Wiley-Interscience, Chichester, 1980; B. F. G. Johnson and R. E. Benfield, *Topics Stereochem.*, 1981, **12**, 253; K. C. C. Kharas and L. F. Dahl, *Adv. Chem. Phys.*, 1988, **70** (Part 2), 1; P. Chini, G. Longoni, and V. G. Albano, *Adv. Organomet. Chem.*, 1976, **14**, 285.
3 M. O. Albers, D. J. Robinson, and N. J. Colville, *Coord. Chem. Rev.*, 1986, **69**, 127.
4 (*a*) G. P. Elliott, J. A. K. Howard, T. Mise, I. Moore, C. M. Nunn, and F. G. A. Stone, *J. Chem. Soc., Dalton Trans.*, 1986, 2091; (*b*) S. J. Davies, G. P. Elliott, J. A. K. Howard, C. M. Nunn, and F. G. A. Stone, *ibid.*, 1987, 2177; (*c*) G. P. Elliott, J. A. K. Howard, T. Mise, C. M. Nunn, and F. G. A. Stone, *ibid.*, p. 2189; (*d*) S. J. Davies and F. G. A. Stone, *ibid.*, 1989, 785; (*e*) S. J. Davies and F. G. A. Stone, unpublished work.
5 P. E. Kreter and D. W. Meek, *Inorg. Chem.*, 1983, **22**, 319.
6 S. J. Davies, J. A. K. Howard, M. U. Pilotti, and F. G. A. Stone, *J. Chem. Soc., Chem. Commun.*, 1989, 190.
7 P. E. Garrou, *Chem. Rev.*, 1981, **81**, 229; A. J. Carty, *ACS Symp. Ser.*, 1982, **196**, 163.
8 A. M. Arif, D. J. Chandler, and R. A. Jones, *Organometallics*, 1987, **6**, 506.
9 J. A. Abad, L. W. Bateman, J. C. Jeffery, K. A. Mead, H. Razay, F. G. A. Stone, and P. Woodward, *J. Chem. Soc., Dalton Trans.*, 1983, 2075; J. A. Abad, E. Delgado, M. E. Garcia, M. J. Grosse-Ophoff, I. J. Hart, J. C. Jeffery, M. S. Simmons, and F. G. A. Stone, *ibid.*, 1987, 41.
10 J. C. Jeffery, C. Marsden, and F. G. A. Stone, *J. Chem. Soc., Dalton Trans.*, 1985, 1315.
11 P. M. Shulman, E. D. Burkhardt, E. G. Lundquist, R. S. Pilato, G. L. Geoffroy, and A. L. Rheingold, *Organometallics*, 1987, **6**, 101.
12 M. J. Chetcuti, P. A. M. Chetcuti, J. C. Jeffery, R. M. Mills, P. Mitrprachachon, S. J. Pickering, F. G. A. Stone, and P. Woodward, *J. Chem. Soc., Dalton Trans.*, 1982, 699.
13 M. Green, J. A. K. Howard, A. P. James, C. M. Nunn, and F. G. A. Stone, *J. Chem. Soc., Dalton Trans.*, 1987, 61.
14 S. V. Hoskins, A. P. James, J. C. Jeffery, and F. G. A. Stone, *J. Chem. Soc., Dalton Trans.*, 1986, 1709.
15 G. L. Geoffroy and S. I. Bassner, *Adv. Organomet. Chem.*, 1988, **28**, 1.
16 L. J. Farrugia, J. C. Jeffery, C. Marsden, P. Sherwood, and F. G. A. Stone, *J. Chem. Soc., Dalton Trans.*, 1987, 51.
17 T. P. Kee, V. C. Gibson, and W. Clegg, *J. Organomet. Chem.*, 1987, **325**, C14.
18 V. C. Gibson, C. E. Graimann, P. M. Hare, M. L. H. Green, J. A. Bandy, P. D. Grebenik, and K. Prout, *J. Chem. Soc., Dalton Trans.*, 1985, 2025.
19 S. Rosenberg, R. R. Whittle, and G. L. Geoffroy, *J. Am. Chem. Soc.*, 1984, **106**, 5934.
20 K. Knoll, G. Huttner, L. Zsolnai, O. Orama, and M. Wasiucionek, *J. Organomet. Chem.*, 1986, **310**, 225.
21 A. G. Orpen, L. Brammer, F. H. Allen, O. Kennard, D. G. Watson, and R. Taylor, *J. Chem. Soc., Dalton Trans.*, in the press.
22 R. Appel, F. Knoll, and I. Ruppert, *Angew. Chem., Int. Ed. Engl.*, 1981, **20**, 731.
23 G. Becker, W. A. Herrmann, W. Kalcher, G. W. Kriechbaum, C. Pahl, C. T. Wagner, and M. L. Ziegler, *Angew. Chem., Int. Ed. Engl.*, 1983, **22**, 413.
24 W. Uedelhoven, K. Eberl, and F. R. Kreissl, *Chem. Ber.*, 1979, **112**, 3376.
25 G. M. Sheldrick, SHELXTL System of programs for use with the Nicolet *X*-ray system, Cambridge, 1976; updated Göttingen, 1981.
26 'International Tables for *X*-Ray Crystallography,' Kynoch Press, Birmingham, 1975, vol. 4.

Received 7th October 1988; *Paper* 8/04002H